Trajectory Generation and Dynamic Control of Planar Biped Robots With Curved Soles

Je Sung Yeon, Ohung Kwon
Department of Precision Mechanical Engineering, Hanyang University, 17 Haengdang-Dong, Sungdong-Ku, Seoul 133-791, Korea
Jong Hyeon Park*
School of Mechanical Engineering, Hanyang University, 17 Haengdang-Dong, Sungdong-Ku, Seoul 133-791, Korea

This paper proposes a locomotion pattern and a control method for biped robots with curved soles. First, since the contact point of a supporting leg may arbitrarily move back and forth on the ground, we derived the desired trajectory from a model called the Moving Inverted Pendulum Model (MIPM) where the Zero Moment Point (ZMP) exists at the supporting point and can be moved intentionally. Secondly, a biped robot with curved soles is an under-actuated system since the supporting point contacting with a point on the ground has no actuator during the single supporting phase. Therefore, this paper proposes a computed-torque control for this under-actuated system using decoupled dynamic equations. A series of computer simulations with a 7-DOF biped robot with curved soles shows that the proposed walking pattern and control method are effective and allow the biped robot to walk fast and stably, and move more like human beings. Also, it is shown that the curved sole shape has superior energy consumption compared to flat soles, and greater efficiency in ascending and descending the stairs.

Key Words: Biped Robot, Curved Soles, Underactuated System, MIPM, Dynamic Control

1. Introduction

Most researchers have studied walking biped robots with flat soles in various artificial environments. However, these biped robots have an unnatural, restrictive and inefficient walking motion when their soles touch the ground. Therefore, some researchers have studied human-like walking motions using biped robots with a toe joint in each foot since toes have a very important role in the walking pattern of human beings (Rose and Gamble, 1981). Specifically, the function or role of a toe's joints is summarized in three aspects. One is utilizing them to speed up walking, another is using them to enable a biped robot to go up higher steps, and the other is using them to make a whole-body action where the knee joints can contact the ground.

In previous works, robotic toe joints were used as both passive joints and active joints. In case of a biped robot with flat soles attached with passive toe joints, its heel contacts first and then its toe takes off as though its toe-tip is hinged to the ground (Nishiwaki et al., 2002). This is called ballistic walking like a projectile moving through space during a single supporting phase (Schiehlen, 2005) and has non-holonomic constraints. Next, biped robots with flat soles attached with active toe joints walk more actively (Takahashi and Kawamura, 2002). However, they require more actuators and have many difficult problems, such as the increase in weight, actuation redundancy

* Corresponding Author,
E-mail : jongpark@hanyang.ac.kr
TEL : +82-2-2220-0435; **FAX** : +82-2-2290-4634
School of Mechanical Engineering, Hanyang University, 17 Haengdang-Dong, Sungdong-Ku, Seoul 133-791, Korea. (Manuscript **Received** May 12, 2005; **Revised** February 24, 2006)

and trajectory generation.

On the other hand, some researchers have studied biped robots with curved soles that do not need to add any additional actuators. They can move into natural and human-like walking patterns using curved soles that cannot be fixed on the ground, but must be rotated continuously from their heel to their toe in order to walk forward. This approach was first suggested by McGeer. He suggested passive dynamic walking for biped robots with curved soles, that is, given only a downhill slope as a source of energy, a human-like pair of legs settles into a natural gait generated by passive interaction of gravity and inertia (McGeer, 1990a ; 1990b). Another work proposed a self-excited biped walking mechanism (One et al., 2000). The curved soles can roll smoothly and steadily along a level surface, maintaining any speed without loss of energy during the supporting phase. However, these works cannot be applied to multi-body robots walking on different surfaces.

In general, there are some problems in the walking control of many DOF biped robots with curved soles on various surfaces. In the single supporting phase, the supporting foot contacting with one point on the ground has no actuator. Thus, the number of actuators is smaller than that of independent configurable variables to control the biped robot. Hence, the biped robot is limited by an under-actuated system. Therefore, the problem of under-actuatiom must be solved in order to control a biped robot with curved soles.

One method for the control law of an under-actuated biped robot is based on the definition of the reference trajectory for outputs, not as a function of time, but as a function of a configurable variable independent of the outputs (Aoustin and Formal'sky, 1999). With such a control, the configuration of the robot at the impact moment is replaced by the desired configuration. This leads to a velocity discontinuity since the actual velocities can differ from the desired velocities. Next, parameterized reference trajectories are introduced. Thus, one derivative of the parameter satisfied with some constraints from the relation between the feet and the ground is used as a supplementary input (Chevallereau and Adouane, 2002). However, these works do not consider the stable walking for multi-body biped robots in various artificial environments.

This paper proposes a computed-torque control for this under-actuated system to control using the decoupled dynamic equations. With such a control, one of independent configurable variables is controlled indirectly. And considering that a supporting foot rotates on the ground, the desired trajectory is derived based on the Moving Inverted Pendulum Model (MIPM). The trajectories are modified to prevent a velocity discontinuity at the contacting moment of a swinging foot.

This paper is organized as follows : Section 2 describes the model of a biped robot with curved soles and the dynamic equations. In order to get the desired trajectory of a biped robot with curved soles, we have made a model called the Moving Inverted Pendulum Model (MIPM) in Sec. 3. It is similar to the Linear Inverted Pendulum Mode (Kim and Park, 1999 ; Park and Cho, 2000). However, robot's supporting point moves horizontally. Section 4 describes the control variables and modified dynamic equations to solve the under-actuated problems. The effectiveness of the proposed control through various computer simulations of a biped robot with curved soles is shown in Sec. 5, followed by conclusions in Sec. 6.

2. Dynamics of a Biped Robot and Its Environment

2.1 Dynamics of a biped robot

A walking cycle is divided into two phases : a single support phase and an instantaneous double supporting phase. Figure 1 shows the structure of a biped robot with curved soles in the sagittal plane. This robot is similar to a 7-DOF biped robots with flat soles. It is composed of a trunk and two identical legs. Each leg is composed of three links that include curved sole. The ankles, knees and hip are one-degree-of-freedom rotational joints. We assume that all links are massive and rigid. And the supporting point of a supporting foot does not rebound and slip.

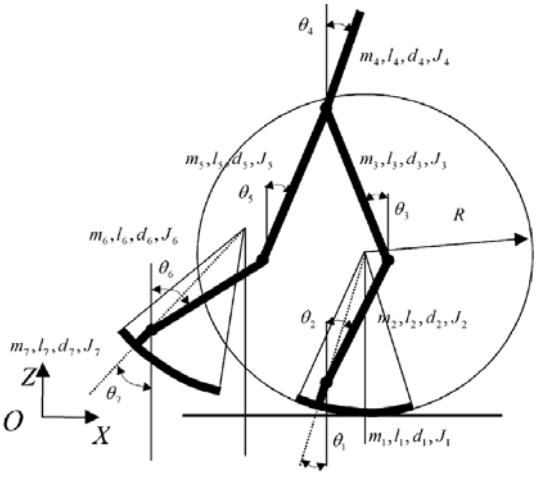

Fig. 1 A biped robot with curved soles and its coordinates

The vector $q=[\theta_1\ \theta_2\ \theta_3\ \theta_4\ \theta_5\ \theta_6\ \theta_7]^T$ describes the configuration of a biped robot in the absolute coordinates. And the mass and the moment of inertia of each link are m_i and I_i, respectively. The length to the center of mass is d_i and the radius of the curved sole is R.

Dynamic equations for this model are obtained by solving Lagrange's equation. Lagrange's equation relates to the angular acceleration of each joint and the applied torque of each actuator; then it is convenient to obtain a nonlinear state space model, taking the angular positions and velocities as state variables.

In the single support phase, the dynamic equation can be written as

$$M(q)\,\ddot{q}+C(q,\,\dot{q})\,\dot{q}+G(q)=PT \qquad (1)$$

where $M(7\times7)$ is the inertia matrix, $C(7\times7)$ is the vector related to the Coriolis and centrifugal forces, and $G(7\times1)$ is the vector of gravity effects. T is a (6×1) torque vector and P is a (7×6) transformation matrix.

$$P=\begin{bmatrix}-1&0&0&0&0&0\\1&-1&0&0&0&0\\0&1&-1&0&0&0\\0&0&1&-1&0&0\\0&0&0&1&-1&0\\0&0&0&0&1&-1\\0&0&0&0&0&1\end{bmatrix},\quad T=\begin{bmatrix}\tau_1\\\tau_2\\\tau_3\\\tau_4\\\tau_5\\\tau_6\end{bmatrix} \qquad (2)$$

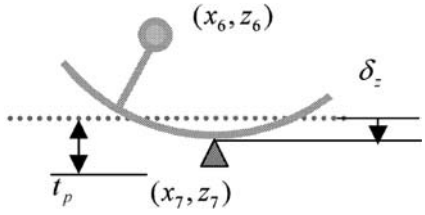

Fig. 2 Environment model

For the instantaneous double supporting phase, the dynamic model can be written as

$$M(q)\,\ddot{q}+C(q,\,\dot{q})\,\dot{q}+G(q)+J^TF=PT \qquad (3)$$

where J is the Jacobian matrix and F is the external force vector.

2.2 Environment model

In order to compute the vertical force when the foot of the freely swinging leg makes an initial contact with the ground, we used the nonlinear spring-damper model, proposed by Park and Kwon (2001), as an environment model for a biped robot with curved soles as shown in Fig. 2. Where (x_6, z_6) and (x_7, z_7) denote the position of the ankle and the position of the contact point, respectively.

An environment model is composed of a nonlinear damper and a linear spring at the supporting point. The vertical force, f_z, generated into the vertical direction is expressed by

$$f_z(\delta_z)=\frac{3}{2}\alpha k_z(\delta_z)\,\delta_z\dot{\delta}_z+k_z(\delta_z)\,\delta_z \qquad (4)$$

where δ_z is the amount of the deformation, $k_z(\delta_z)$ is the stiffness, and α is a constant that defines the relation between the coefficient of restitution and the impact velocity.

Generally, in order to provide more realistic environmental forces, the springs have nonlinear stiffness characteristics such as

$$k_z(\delta_z)=k_0\left[1+0.1\tan^3\left(\frac{\pi\delta_z}{2t_p}\right)\right] \quad \text{for } \delta_z>0 \qquad (5)$$

where k_0 is the stiffness associated with the spring model along the z-axis, and t_p is the maximum deformable height.

3. Trajectory Generation

Commonly, periodic walking trajectories of a biped robot are derived from the Linear Inverted Pendulum Mode (LIPM) or the Gravity-Compensated Inverted Pendulum Mode (GCIPM) under the assumption that the ZMP exists in the center of a robot foot in the supporting phase. It is assumed that most of the weight of the biped robot is concentrated on one or two particles and the contact point is fixed. And the trajectories with respect to the center of mass and a swing foot are specified.

For biped robots with curved soles, the supporting point moves into the horizontal direction. Thus, we do not use the LIPM or the GCIPM to generate the trajectory of the biped robot with curved soles. Therefore, we propose the new trajectory called the Moving Inverted Pendulum Model (MIPM). It has an advantage that we can move the ZMP position arbitrarily because the supporting point of a supporting leg is the ZMP position.

3.1 Moving inverted pendulum model (MIPM) for the supporting leg

The MIPM is based on a simple biped model that is approximated into one particle, assuming that most of the weight of the biped robot is concentrated on its hip link, but the supporting point moves arbitrarily. Figure 3 shows the one-particle model for the MIPM. Where Vectors $\vec{p}_1$ and $\vec{p}_2$ are the vector from the origin of the reference frame, O, to the supporting point, A, and the vector from the supporting point, A, to the center of mass, M, respectively. And ϕ and g are the slope angle of the center of mass about the vertical axis and the gravity acceleration, respectively.

Newton's second law says that the sum of the moments about O induced from all the forces acting on the particle is equal to the rate of change of the moment of momentum, or the angular momentum, of the particle about O.

$$\sum M_o = \dot{H}_o \tag{6}$$

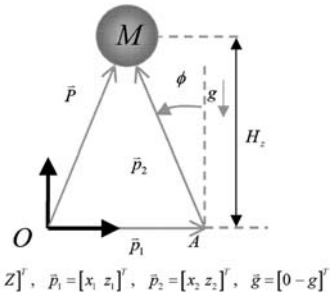

Fig. 3 Moving Inverted Pendulum Model (MIPM)

The angular momentum with respect to the fixed coordinate O as shown in Fig. 3 is derived as

$$\vec{H}_o = \vec{P} \times M\dot{\vec{P}} = (\vec{p}_1 + \vec{p}_2) \times M(\dot{\vec{p}}_1 + \dot{\vec{p}}_2) \tag{7}$$

If differentiating Eq. (7),

$$\begin{aligned} \dot{\vec{H}}_o &= (\dot{\vec{p}}_1 + \dot{\vec{p}}_2) \times M(\dot{\vec{p}}_1 + \dot{\vec{p}}_2) \\ &\quad + (\vec{p}_1 + \vec{p}_2) \times M(\ddot{\vec{p}}_1 + \ddot{\vec{p}}_1) \\ &= M[x_1 + x_2,\ z_1 + z_2]^T \times [\ddot{x}_1 + \ddot{x}_2,\ \ddot{z}_1 + \ddot{z}_2]^T \end{aligned} \tag{8}$$

where it is assumed that the robot moves only in the sagittal plane and the height of the center of mass remains constant; $z_1=0$, $z_2=H_z$. Therefore, the rate of change of the angular momentum is derived as follows:

$$\dot{\vec{H}}_o = MH_z(\ddot{\vec{x}}_1 + \ddot{\vec{x}}_2) \tag{9}$$

The moment about O is

$$\begin{aligned} \vec{M}_0 &= \vec{P} \times M\vec{g} - \vec{p}_1 \times M\vec{g} \\ &= M(\vec{p}_1 + \vec{p}_2) \times \vec{g} - \vec{p}_1 M\vec{g} \\ &= M[x_1 + x_2 \quad z_1 + z_2]^T \times [0 \quad -g]^T \\ &\quad - M[x_1 \quad z_1]^T \times [0 \quad -g]^T = Mgx_2 \end{aligned} \tag{10}$$

If inserting Eqs. (9) and (10) into Eq. (6), we get a simple equation that describes the dynamic motion along x-axis.

$$\begin{aligned} MH_z(\ddot{x}_1 + \ddot{x}_2) &= Mgx_2 \\ \ddot{x}_1 + \ddot{x} &= \frac{g}{H_z} x_2 \end{aligned} \tag{11}$$

where x_1 and x_2 are the functions of the slope angle, ϕ, from the kinematic relation. And it is assumed that $\tan\phi$ is almost equal to ϕ on condition that ϕ is less than $\pi/10$.

$$\begin{aligned} x_1 &= x_1(0) + R(\phi(0) - \phi) \\ x_2 &= -H_2 \tan\phi \approx -H_z\phi \quad (|\phi| < \pi/10) \end{aligned} \tag{12}$$

where $x(0)$ and $\phi(0)$ is the initial values at time $t=0$.

If inserting Eq. (12) into Eq. (11), a second-order differential equation is obtained as follows:

$$\ddot{\phi}=\omega^2\phi,\ \omega=\sqrt{\frac{g}{H_z+R}} \tag{13}$$

The corresponding general solution is

$$\begin{aligned}&\phi(t)=C_1e^{\omega t}+C_2e^{-\omega t}\\&C_1=\frac{1}{2}\left\{\phi(0)+\frac{\dot{\phi}(0)}{\omega}\right\},\ C_2=\frac{1}{2}\left\{\phi(0)-\frac{\dot{\phi}(0)}{\omega}\right\}\end{aligned} \tag{14}$$

Equation (14) should be satisfied with the repeatability conditions, that is, $\phi(0)=-\phi(T)$ and $\dot{\phi}(0)=\dot{\phi}(T)$. Since locomotion is periodic, and the speed and configuration of the left and right legs at the end of the stride become identical to those of the right and left legs respectively at the beginning of the stride. Therefore, the initial velocity of the slope angle can be found as follows:

$$\dot{\phi}(0)=\frac{1+e^{\omega T}}{1-e^{\omega T}}\omega\phi(0) \tag{15}$$

Therefore, desired trajectories, $(X,\ Z)$, of the center of mass are derived as

$$\begin{aligned}X&=x_1+x_2=x_1(0)+R(\phi(0)-\phi)-H_z\phi\\&=-(R+H_z)\phi+x_1(0)+R\phi(0)\\Z&=z_1+z_2=H_z\end{aligned} \tag{16}$$

where the desired vertical trajectory of the center of mass is set to be constant in the process of deriving the horizontal trajectory of the center of mass. But for human-like, efficient walking, the desired vertical trajectory of the center of mass is used as the following equation (McMahon, 1984).

$$Z=H_z+H_z\left(1-\cos\left(\frac{S}{2H_z}\right)\right)\sin\left(\frac{\pi}{T}t\right),\quad 0\le t\le T$$

where S is the stride and T is the one step period.

3.2 Trajectory generation for the free leg

The foot trajectories with respect to the position of the ankle joint, $(x_f,\ z_f)$, and the rotation angle of the swing foot about the absolute coordinates, θ_f, are specified. First, ankle trajectories

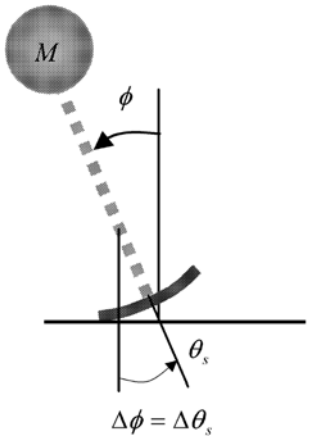

Fig. 4 The relation between ϕ and θ_s in the MIPM

are used as follows:

$$\begin{aligned}&x_f(t)=x_s-S\cos\{\omega_f t\}\qquad(0\le t\le T)\\&z_f(t)=\frac{h_f}{2}[1-\cos\{2\omega_f t\}]\quad\omega_f=\pi/T\end{aligned} \tag{17}$$

where h_f is the maximum foot height and x_s is the position of a supporting leg.

Based on the assumption that the rate of change of the slope angle of the center of mass is equal to the rate of change of the foot angle of the supporting leg as shown in Fig. 4, the foot angle θ_s of the supporting leg is derived as

$$\begin{aligned}&\Delta\theta_s=\Delta\phi\\&\theta_s=\phi-\phi(0)+\theta_s(0)\end{aligned} \tag{18}$$

where $\theta_s(0)$ and $\phi(0)$ are initial values.

The foot angle of the swing leg, θ_f, is connected continuously into the foot angle of the supporting leg, θ_s, in order to walk periodically. Therefore, we use a third order polynomial.

$$\theta_f=At^3+Bt^2+Ct+D \tag{19}$$

where this polynomial should be satisfied with the continuity conditions.

$$\begin{aligned}&\theta_f(0)=\theta_s(T),\ \theta_f(T)=\theta_s(0)\\&\dot{\theta}_f(0)=\dot{\theta}_s(T),\ \dot{\theta}_f(T)=\dot{\theta}_s(0)\end{aligned}$$

3.3 Modified trajectory generation for the free leg

A swing leg has initial errors at the start of the supporting phase because a supporting point has no actuator and rotates around a supporting

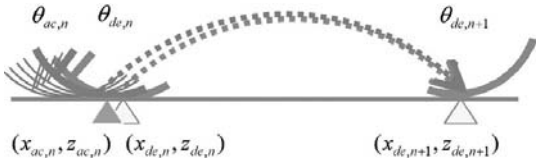

Fig. 5 Modification of the swing leg trajectory

point on the ground, and this rotation makes the supporting foot translate largely as shown in Fig. 5. Where the subscript 'ac' and 'de' mean the actual data and the desired data at n-th walking cycle, respectively. These initial errors largely don't affect the stability if they exist inside the limit range when a swing leg starts with the supporting phase. But they become larger over the limit range after some periods. Therefore, a swing foot trajectory is modified to satisfy the initial conditions at the moment the swing phase starts with each step.

First, the swing leg trajectory (x_f', z_f') is modified from Eq. (16).

$$x_f'(t)=x_{ac,n}-S'[1-\cos(\omega_f t)]\quad S'=\frac{x_{de,n+1}-x_{ac,n}}{2}$$
$$z_f'(t)=\frac{h_f}{2}[1-\cos(2\omega_f t)]\qquad \omega_f=\frac{\pi}{T} \tag{20}$$

where $x_{ac,n}$ is the actual ankle position of a supporting foot at n-th step.

The modified foot angle of a swing leg, θ_f', is connected continuously into the modified foot angle of a supporting leg, θ_s', in order to walk periodically. Similarly, we use a third order polynomial.

$$\theta_f'=A't^3+B't^2+C't+D' \tag{21}$$

where this polynomial should be satisfied with the continuity conditions.

$$\theta_f'(0)=\theta_{ac,n}(T),\ \theta_f'(T)=\theta_{de,n+1}(0)$$
$$\dot\theta_f'(0)=\dot\theta_{ac,n}(T),\ \dot\theta_f'(T)=\dot\theta_{de,n+1}(0)$$

4. Control Design for the Underactuated System

The sole of the supporting leg contacts the floor as a point. This non-actuated point is a free joint that cannot easily balance the robot's body and stabilize the robot's motions. Thus, it is difficult to control the body position and posture because this system is an under-actuated system. The degree of under-actuation is one. Therefore, this paper presents a control method for this under-actuated system to track cyclic reference trajectories, based upon the computed-torque control.

4.1 Control design

Dynamic equations can be divided into two parts : the equations related directly to torque and the equations related indirectly to torque. In this paper, one of seven independent configuration variables can be written as a relation equation independent of the torques since the number of torques is six but there are seven independent configuration variables.

Definition

(1) The transformation matrix P in Eq. (2) is a (7×6) full rank matrix. Thus, there exist a (1×7) matrix $P^\perp$ such that $P^\perp P=0$.

(2) The transformation matrix P in Eq. (2) is not invertible. Thus, its pseudo-inverse P^+ is defined such that $P^+P=I$.

By definition of P^+ and $P^\perp$, the matrix $[P^\perp\ P^+]^T$ is a (7×7) invertible matrix (Chevallereau, 2003). In general, the matrix P is constant. Therefore, P^+ and $P^\perp$ are constant and can be calculated offline.

If dividing dynamic equations in Eq. (2) into two parts, the following set of equations is described as :

$$P^\perp(M(q)\ddot q+C(q,\dot q)\dot q+G(q)+J^TF)=0 \tag{22}$$

$$P^+(M(q)\ddot q+C(q,\dot q)\dot q+G(q)+J^TF)=T \tag{23}$$

In order to obtain input torques from these dynamic equations, we have to eliminate one parameter using the equation unrelated to the torques. If a relation equation independent of the torques are written with respect to the joint angle of a supporting foot, θ_1, the following equation is obtained from Eq. (22).

$$\ddot\theta_1=f(\ddot q,\dot q,q) \tag{24}$$

where $f(\cdot)$ is a function except $\ddot{\theta}_1$.

The configurable variable vector $q=[\theta_1\ \theta_2\ \theta_3\ \theta_4\ \theta_5\ \theta_6\ \theta_7]^T$ describes the configuration of a biped robot in the absolute coordinates. These variables are reduced in number from seven to six since the number of actuators is smaller than that of independent configurable variables. Therefore, in order to apply to the computed torque control, control variables with respect to the error dynamics are defined as follows: hip position (x_h, z_h), ankle position of the swing leg (x_a, z_a), joint angle of the upper body (θ_t), and ankle joint angle of the swing leg (θ_f). Thus, they are described as a variable vector, r.

$$q=[\theta_1\ \theta_2\ \theta_3\ \theta_4\ \theta_5\ \theta_6\ \theta_7]^T$$
$$\Rightarrow r=[x_h\ z_h\ x_a\ z_a\ \theta_t\ \theta_f]^T$$

This transformation means that just one independent configuration variable must be controlled indirectly.

Using Eq. (24) and the kinematic relation between r and q, the error dynamics is defined as the following equation.

$$\begin{aligned}\dot{r}&=\dot{r}_d+k_v(\dot{r}-\dot{r}_d)+k_p(r-r_d)\\&=A[\ddot{\theta}_2\ \ddot{\theta}_3\ \ddot{\theta}_4\ \ddot{\theta}_5\ \ddot{\theta}_6\ \ddot{\theta}_7]^T+B\end{aligned}\tag{25}$$

where k_v and k_p are the gain matrices and the joint errors are asymptotically stable under the assumption that there does not exist a little parameter uncertainty. And A and B are the transformation matrices related to each joint angle and angular velocity.

If transforming Eq. (25) into a angular acceleration vector,

$$[\ddot{\theta}_2\ \ddot{\theta}_3\ \ddot{\theta}_4\ \ddot{\theta}_5\ \ddot{\theta}_6\ \ddot{\theta}_7]^T=A^{-1}(-B+\dot{r})\tag{26}$$

And if inserting Eq. (26) into Eq. (22), the modified $\ddot{\theta}_1$ minimizing tracking errors is obtained.

$$\ddot{\theta}_1=f_1(\ddot{q},\ \dot{q},\ q)\tag{27}$$

where $f_1(\cdot)$ is a function except $\ddot{\theta}_1$.

If inserting Eqs. (26) and (27) into Eq. (23), input torques are obtained.

$$\begin{aligned}T=&P^+(M(q)[f_1(\cdot)\ \ (A^{-1}(-B+\dot{r}))^T]^T\\&+C(q,\ \dot{q})\dot{q}+G(q)+J^TF)\end{aligned}\tag{28}$$

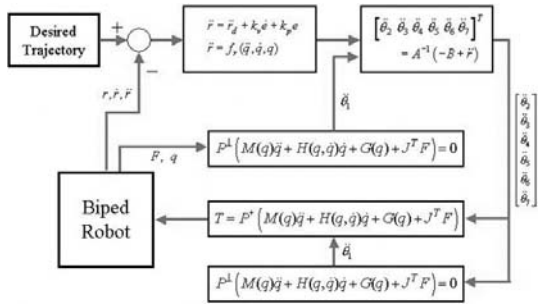

Fig. 6 A flow chart of the control algorithm

where the external force F occurs when a swing foot contacts to the ground.

Figure 6 is a flow chart of the control algorithm. The angular acceleration, $\ddot{\theta}_1$, is eliminated using the equation unrelated to the torques as shown in Eq. (24). And then a function composed of $\ddot{\theta}_2$, $\ddot{\theta}_3$, $\ddot{\theta}_4$, $\ddot{\theta}_5$, $\ddot{\theta}_6$, $\ddot{\theta}_7$ is obtained. This function is inserted into the equation related to the torques as shown in Eq. (23). As a result, we can obtain the input torque vector and control a biped robot with curved soles.

5. Simulation

The effectiveness and the performance of the proposed dynamic control are shown in computer simulations. It is assumed that the center of gravity of each link is known and fixed at the center of the link. The physical parameters of a biped robot with curved soles used in this simulation are listed in Table 1. And the parameters used in the MIPM are listed in Table 2. Where x_1 is the position of a supporting leg and γ is the distance translated by the rotation of the curved sole in a supporting leg. In the simulation, α=05, k_o=10000 N/m, t_p=0.001 m, R=0.3 m.

Figure 7 shows a stick diagram for normal walking of a biped robot with curved soles on a flat surface. Where sticks and small circles are links and joints, respectively. And its hip joint moves up and down. The trajectories of each joint angle are shown in Fig. 8. These figures show that the biped robot walks continuously because the proposed controller reduces tracking errors and the initial errors of a swing foot are modified at

Table 1 Physical parameters of the biped model used

Link	1	2	3	4	5	6	7
Length (m)	0.05	0.35	0.35	0.3	0.35	0.35	0.05
Mass (kg)	1	1	1	6	1	1	1

Table 2 Locomotion parameters used in the MIPM

Parameters	Symbol	Values
Step time	T	0.5 sec
Height of the center of mass	H_z	0.7 m
Stride	$S+(x_1(T)-x_1(0))$	$0.2+\gamma$ m
Maximum foot height	h_f	0.05 m

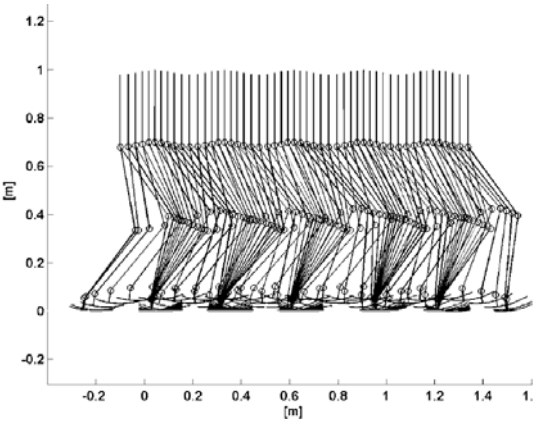

Fig. 7 Stick diagram of a biped robot walking on flat surface in the sagittal plane

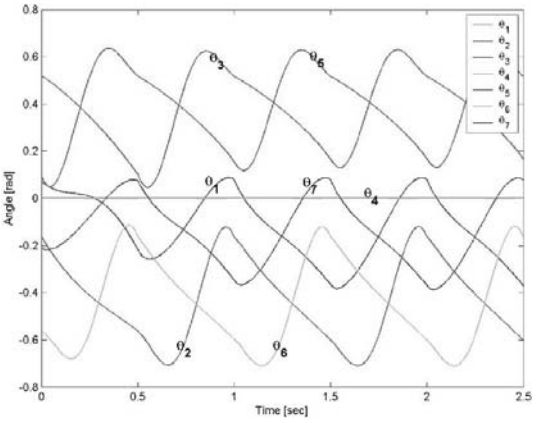

Fig. 8 Trajectory of each joint angle

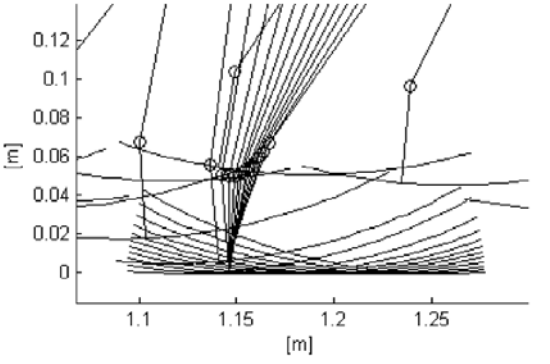

Fig. 9 Stick diagram of a supporting foot in the sagittal plane

the starting moment of the swing phase.

Figure 9 shows that a supporting foot with a curved sole rolls on the ground and its contact point moves on the horizontal surface. This rotation motion makes the stride longer almost 10 cm to 15 cm. This means that the stride of a biped robot with curved soles (when the radius of the curved sole R is 0.3 m ($R=0.3m$)) showing a more 25% to 37% increase compared to that of a biped robot with flat soles (when the radius of the curved sole R is infinity ($R=\infty$) and also its ankle joint can move within the range limit of 3.5 cm in x-axis and 2 cm in z-axis. This rotation helps to avoid singular conditions at walking on the ground or going up stairs and is also useful with respect to energy efficiency because the 7-dof biped walking mechanism possesses and uses passive curved feet like passive dynamic walking on a downhill slope studied by McGeer (1990). Figure 10 shows that the curved sole is more efficient than the flat sole with the same stride. Thus, the consumption power is reduced by 36%. Figure 11 shows a stick diagram for walking a staircase in the sagittal plane. Visually two feet of the biped robot with curved soles have very natural motion. In addition, its knee joint is stretched almost in the same way as the walking pattern of a human being.

High speed walking of a biped robot with flat soles requires the knee joint to be stretched to its limit and an increase in stride per a step. In general, this results in kinematic singularity as the stride lengthens. However, simulation results with

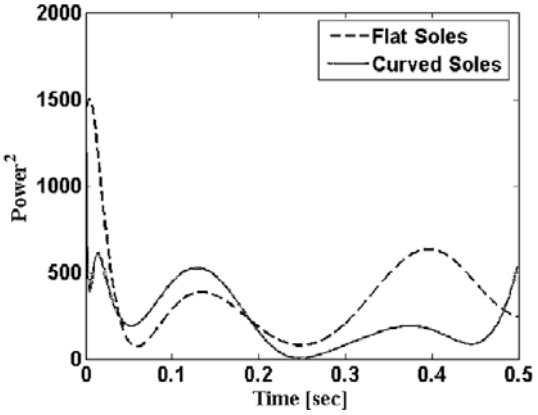

Fig. 10 Energy comparison in a viewpoint of the sole shape

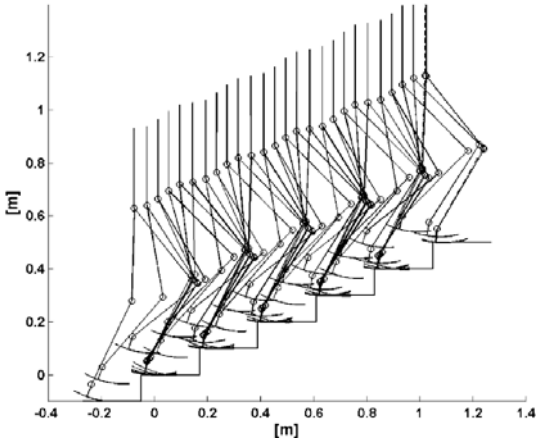

Fig. 11 Stick diagram of a biped robot walking a staircase in the sagittal plane

respect to high speed walking show that a biped robot with curved soles can walk stably and quickly without stretching its leg because the curved sole has the same effect as a dynamic link whose length changes.

In the field of biped robots, periodic and stable walking is the one of the most important issues. Figure 12 shows the phase portraits with respect to each joint angle and each joint angular velocity for 50 steps. They display oscillations of fixed amplitude and fixed period, that is, limit cycles. When the robot starts to walk, its motion exists outside the limit cycles. But after some steps, its motion can neither grow unbounded nor decay to zero. Instead, it converges into limit cycles. These

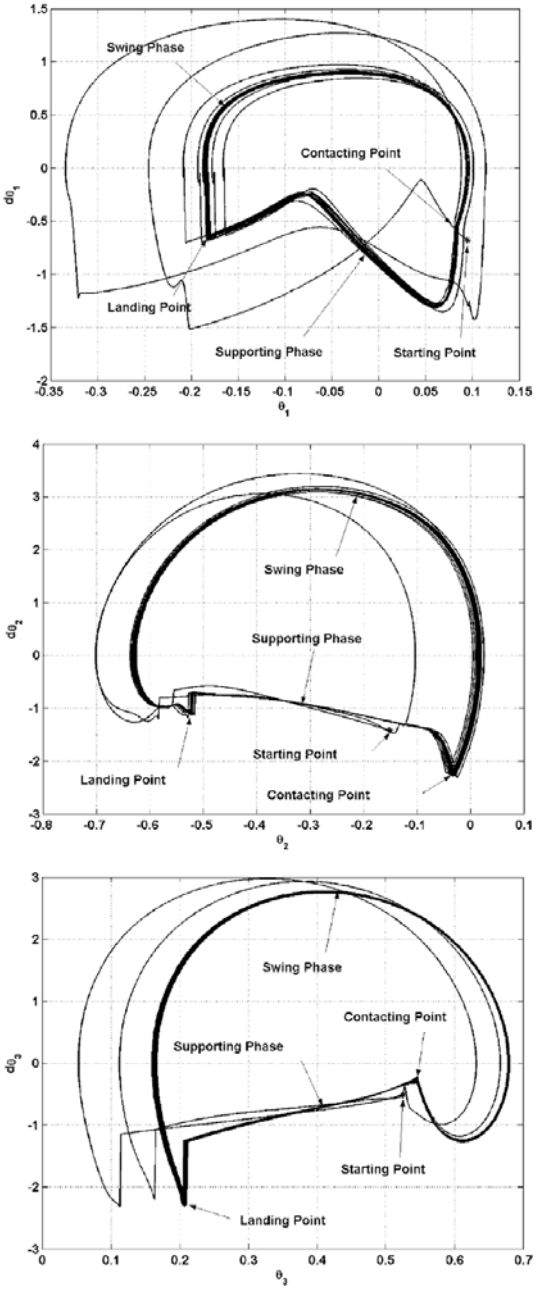

Fig. 12 Phase portraits of each joint

limit cycles indicate stable walking of the biped robot with curved soles.

6. Conclusion

This paper proposed a control method and a

trajectory generation method for biped robots with curved soles in order to get the same effectiveness as toe joints without requiring extra actuators. Thus, we derived the desired trajectory with the Moving Inverted Pendulum Model and controlled the under-actuated system. Computer simulation results showed that a biped robot with curved soles walks stably although periodic errors occur. The position translation of its ankle joint by the rotation of its curved sole at contacting on the ground is an important difference, compared to biped robots with flat soles. It is also effective for walking up-and-down stairs.

References

Aoustin, Y. and Formal'sky, A. M., 1999, "Design of Reference Trajectory to Stablilize Desired Nominal Cyclic Gait of a Biped," *IEEE Robot Motion and Control*, pp. 159～164.

Chevallereau, C. and Adouane, L., 2002, "On-line Reference Trajectory Adaptation for the Control of a Planar Biped," *Conf. Climbing and Walking Robots*, pp. 427～436.

Chevallereau, C., 2003, "Time-Scaling Control for a Underactuated Biped Robot," *IEEE Transactions on Robotics and Automation*, Vol. 19, No. 2, pp. 362～368.

Kim, K. D. and Park, J. H., 1999, "Biped Robot Locomotion and Control Using Gravity-Compensated Inverted Pendulum Mode," *KSME Journal*, Vol. 23, No. 2, pp. 209～216.

McMahon, T. A., 1984, *Muscles, Reflexes, and Locomotion*, Princeton University Press.

McGeer, T., 1990, "Passive Dynamic Walking," *The International Journal of Robotics Research*, Vol. 9, No. 2, pp. 62～82.

McGeer, T., 1990, "Passive Walking with Knees," *IEEE Int. Conf. on Robotics and Automation*, pp. 1640～1645.

Nishiwaki, K., Kagami, S., Kuniyoshi, Y., Inaba, M. and Inoue, H., 2002, "Toe Joints that Enhance Bipedal and Fullbody Motion of Humanoid Robots," *IEEE Int. Conf. on Robotics and Automation*, pp. 3105～3110.

One, K., Takahashi, R., Imadu, A. and Shimada, T., 2000, "Self-Excitation Control for Biped Walking Mechanism," *IEEE Int. Conf. on Intelligent Robots and Systems*, pp. 1143～1148.

Park, J. H. and Cho, H. C., 2000, "An On-Line Trajectory Modifier for the Base Link of Biped Robots To Enhance Locomotion Stability," *IEEE Int. Conf. on Robotics and Automation*, pp. 3353～3358.

Park, J. H. and Chung, H., 1999, "Hybrid Control for Biped Robots Using Impedance Control and Computed-Torque Control," *IEEE Int. Conf. on Robotics and Automation*, pp. 1365～1370.

Park, J. H. and Kwon, O., 2001, "Reflex Control of Biped Robot Locomotion on a Slippery Surface," *IEEE Int. Conf. on Robotics and Automation*, pp. 4134～4139.

Rose, J. and Gamble, J. G., 1981, *Human Walking*, Williams & Wilkins.

Schiehlen, W., 2005, "Recent Developments in Multibody Dynamics," *Journal of Mechanical and Science and Technology*, Vol. 19, No. 1, pp. 227～236.

Takahashi, T. and Kawamura, A., 2002, "Pasture Control using Foot Toe and Sole for Biped Walking Robot 'Ken'," *Int. Workshop on Advanced Motion Control*, pp. 437～442.